Generation of a Novel Functional Neuronal Circuit in *Hoxa1* Mutant Mice

Eduardo Domínguez del Toro,[1] Véronique Borday,[1] Marc Davenne,[2] Rüdiger Neun,[2] Filippo M. Rijli,[2] and Jean Champagnat[1]

[1]*Neurobiologie Génétique et Intégrative, Unité Propre de Recherche 2216, Centre National de la Recherche Scientifique (CNRS), 91198 Gif-sur-Yvette, France, and* [2]*Institut de Génétique et de Biologie Moléculaire et Cellulaire, CNRS/Institut National de la Santé et de la Recherche Médicale/Université Louis Pasteur, Collège de France, BP 163-67404 Illkirch, Centre Universitaire de Strasbourg, France*

Early organization of the vertebrate brainstem is characterized by cellular segmentation into compartments, the rhombomeres, which follow a metameric pattern of neuronal development. Expression of the homeobox genes of the *Hox* family precedes rhombomere formation, and analysis of mouse *Hox* mutations revealed that they play an important role in the establishment of rhombomere-specific neuronal patterns. However, segmentation is a transient feature, and a dramatic reconfiguration of neurons and synapses takes place during fetal and postnatal stages. Thus, it is not clear whether the early rhombomeric pattern of *Hox* expression has any influence on the establishment of the neuronal circuitry of the mature brainstem. The *Hoxa1* gene is the earliest *Hox* gene expressed in the developing hindbrain. Moreover, it is rapidly downregulated. Previous analysis of mouse *Hoxa1* $^{-/-}$ mutants has focused on early alterations of hindbrain segmentation and patterning. Here, we show that ectopic neuronal groups in the hindbrain of *Hoxa1* $^{-/-}$ mice establish a supernumerary neuronal circuit that escapes apoptosis and becomes functional postnatally. This system develops from mutant rhombomere 3 (r3)-r4 levels, includes an ectopic group of progenitors with r2 identity, and integrates the rhythm-generating network controlling respiration at birth. This is the first demonstration that changes in *Hox* expression patterns allow the selection of novel neuronal circuits regulating vital adaptive behaviors. The implications for the evolution of brainstem neural networks are discussed.

Key words: homeobox genes; Hoxa1 knock-out; respiration; suction; rhythm generation; rhombomeres; neural progenitors; migratory pathways; neuronal networks, reticular formation; pons; hindbrain; brainstem; newborn mice

In the hindbrain of the vertebrate embryo, *Hox* genes are segmentally expressed and loss- and gain-of-function mutations revealed their involvement in neuronal patterning (Carpenter et al., 1993; Mark et al., 1993; Goddard et al., 1996; Lumsden and Krumlauf, 1996; Studer et al., 1996; Gavalas et al., 1997, 1998; Helmbacher et al., 1998; Rijli et al., 1998; Bell et al., 1999; Davenne et al., 1999; Jungbluth et al., 1999; Rossel and Capecchi, 1999). Expression of *Hoxa1* is one of the earliest signs of regionalization within the developing hindbrain. As early as 7.5 d postcoitum (dpc), the *Hoxa1* expression domain extends from the posterior end of the mouse embryo up to the presumptive rhombomere 3 (r3)-r4 border and is downregulated before rhombomere boundary formation (Murphy and Hill, 1991). This transient expression has a profound impact on hindbrain patterning, because *Hoxa1*-targeted inactivation results in a severe reduction of r4 and r5 and their derived structures (e.g., the motor nucleus of the facial nerve) and in lethality shortly after birth (Carpenter et al., 1993; Mark et al., 1993). However, it is unclear how transient *Hox* expression before segment formation may influence the generation of functional neuronal networks in the postsegmental hindbrain (Fortin et al., 1999) and affect vital behaviors during postnatal life (Fortin et al., 2000). By examining hindbrain neural networks in *Hoxa1* $^{-/-}$ mice, we now identify ectopic groups of mis-specified neurons that escape apoptosis (Rossel and Capecchi, 1999) during development and control the respiratory rhythm-generating neural network (Champagnat and Fortin, 1996) after birth.

MATERIALS AND METHODS

Mouse lines and genotyping. Hoxa1 mutant mice (Mark et al., 1993), embryos, and newborns were genotyped by PCR as described previously (Gavalas et al., 1998). The r2-*lacZ* transgenic line was obtained by injection of a construct carrying a 2.5 kb *Bam*HI *Hoxa2* genomic fragment (Frasch et al., 1995) cloned in a non-native orientation into the BGZ40 plasmid (Studer et al., 1996), containing the human β-globin

Received Sept. 28, 2000; revised April 11, 2001; accepted May 1, 2001.

Work in J.C.'s laboratory was supported by Human Frontier Science Program Research Grant 101/97, Action Concertée Incitative (Biologie du Développement et Physiologie Intégrative) #57 the Centre National de la Recherche Scientifique, and the Fondation pour la Recherche Médicale (FRM). E.D.T. was supported by The European Community (BIO4-CT975-096) and FRM (EP001227/1) training grants. Work in F.M.R.'s laboratory was supported by the CNRS, the Institut National de la Santé et de la Recherche Médicale, the Hôpital Universitaire de Strasbourg, the Ligue Nationale Contre le Cancer (LNCC), the Association pour la Recherche sur le Cancer, and the Programme Génome du CNRS. M.D. was supported by fellowships from the LNCC and FRM. R.N. was supported by Deutscher Akademischer Austauschdienst and FRM fellowships. We thank P. Chambon, G. Fortin, C. Goridis, R. Krumlauf, and A. Lumsden for valuable discussions and comments on this manuscript. We also thank T. Jacquin for his participation in some *in vitro* experiments and M. Poulet for excellent technical assistance. We acknowledge the following colleagues for kind gifts of reagents: P. Chambon (Hoxa1 mice), R. Krumlauf (BGZ40 plasmid and Hoxb1 probe), and J. F. Brunet (Phox2b probe). The 4D5 antibody was obtained from the Developmental Studies Hybridoma Bank under contract NO1-HD-7-3263.

E.D.T., V.B., and M.D. contributed equally to this work

Correspondence should be addressed to J. Champagnat, Institut de Neurobiologie Alfred Fessard, Centre National de la Recherche Scientifique, Unité Propre de Recherche 2216 (bât. 33), 91198 Gif-sur-Yvette, France. E-mail: Jean.Champagnat@iaf.cnrs-gif.fr.

V. Borday's present address: Laboratoire de Biologie du Développement, Université Paris 7, case 7077, 2 place Jussieu, 75251 Paris, France.

M. Davenne's present address: Cold Spring Harbor Laboratory, 1 Bungtown Road, Cold Spring Harbor, NY 11724.

promoter driving *lacZ* expression. Transgenic r2-*lacZ* mice were bred with *Hoxa1*$^{+/-}$ mice to produce *Hoxa1*$^{+/-}$, r2-*lacZ* animals. The latter were bred with *Hoxa1*$^{+/-}$ animals to produce embryos with the desired genotype. Detection of the transgene was performed by PCR.

Whole-mount in situ *RNA hybridization, immunohistochemistry, and 5-bromo-4-chloro-3-indolyl β-D-galactoside staining.* Whole-mount *in situ* RNA hybridization was performed as described previously (Davenne et al., 1999) using the *Phox2b* (Pattyn et al., 1997) and *Hoxb1* (Studer et al., 1996) probes. Whole-mount immunohistochemistry using the anti-ISL1 monoclonal antibody (4D5) (Developmental Studies Hybridoma Bank, Iowa City, IA) and 5-bromo-4-chloro-3-indolyl β-D-galactoside staining was performed as described previously (Davenne et al., 1999). Hindbrains were dissected out and flat-mounted before being photographed. Postnatal neuronal groups (Jacquin et al., 1996) were identified on coronal, horizontal, and parasagittal 40-μm-thick sections processed alternatively using cresyl violet and polyclonal antibodies to choline acetyltransferase (1:1000 in PBS, pH 7.4; Chemicon, Temecula, CA) and to tyrosine hydroxylase (1:1000 in PBS; Boehringer Mannheim, Mannheim, Germany) in the presence of Triton X-100 and were subsequently revealed using the Vectastain avidin–biotin complex kit (Vector Laboratories, Burlingame, CA) as described previously (Jacquin et al., 1996). To study axonal pathways, the trigeminal motor root or the bulbar reticular area ventral to the ambiguus nucleus was pressure injected with DiI (5 mg/ml in DMSO) after brain fixation. Incubation times (at 37°C) were 3 d after trigeminal injections and 4 d after bulbar injections.

Plethysmograph recordings and naloxone treatment in vivo. We used 231 mice from 34 *Hoxa1* litters. Sixty mice were wild type (WT), 124 mice were heterozygous mutants, and 47 mice were homozygous mutants, a proportion close to the Mendelian expectation. Respiratory activity was measured every 6 hr using a modified barometric method used previously in neonates (Jacquin et al., 1996). The whole-body plethysmograph chamber (20 ml) equipped with a temperature sensor (LN 35 Z) was connected to a reference chamber of the same volume. The pressure difference between the two chambers was measured with a differential pressure transducer (DP 103-12; Validyne, North Ridge, CA) connected to a sine wave carrier demodulator (CD15; Validyne). Neonates were removed individually from the litter and placed in the plethysmograph chamber, which was kept hermetically closed and maintained at 31°C during the recording session (2 min). During quiet breathing, a computer-assisted method was used to measure the duration of inspirations and expirations from which the respiratory frequency is derived. Naloxone was administered (3.33 mg/kg, s.c., in 50 μl of saline) using a Hamilton syringe at the end of the first plethysmographic recording (1–2 hr after birth), and the stimulatory effect on respiration was controlled 0.5–1 hr later.

Network analysis in vitro. The brainstem was removed as described previously (Jacquin et al., 1996, 1999) and cut horizontally (see Fig. 3*F*) under visual control with a vibratome (series 1000; Technical Products International, O'Fallon, MO). The 1200-μm-thick slice was transferred, dorsal side up, into a recording chamber and perfused with artificial CSF, pH 7.4, containing (in mM) 130 NaCl, 5.4 KCl, 0.8 KH_2PO_4, 26 $NaHCO_3$, 30 glucose, 1 $MgCl_2$, and 0.8 $CaCl_2$, saturated with carbogen (90% O_2, 10% CO_2). Motor activities were recorded from the motor trigeminal roots using suction electrodes. Previous experiments (Jacquin et al., 1999) have demonstrated that the respiratory activity *in vitro* propagates to this nerve. The selected root was contralateral to the studied pontine neuronal structure (see Fig. 3*G*) to avoid stimulating directly the recorded motoneurons. Other electrodes were located on the dorsal surface under the visual guidance of a microscope (ACM; Zeiss, Thornwood, NY), and locations were identified histologically. Neurons were recorded in the whole-cell configuration with patch-clamp electrodes as described by Fortin et al. (1999). Electrodes containing 0.1–0.5 mM AMPA in artificial CSF were used for pressure application (0.1 bar, 20 msec). Experiments were performed according to authorization by the ministry of Research Technology and Agriculture, which provides authorization to have the animal facilities.

RESULTS

A supernumerary neuronal structure in the dorsal pons of *Hoxa1*$^{-/-}$ mice

Morphological analysis of the pons at birth indicates a rather extensive cellular reorganization in *Hoxa1*$^{-/-}$ mutants, affecting different cell types. First, in keeping with the heterogeneous anteroposterior (A-P) pattern of the ventricular zone, the anterior fourth ventricle exhibits a characteristic morphological abnormality in newborn mutants (Fig. 1, compare *A–D*). Moreover, the size of the reticular formation is affected both dorsally and ventrally. Ventrally, a 40% reduction in the length of the ventral pons (vP) (Fig. 1*E,F*, *rectangle*) results from the elimination of r4- and r5-derived structures. In contrast, dorsally, a 6% increase in the postnatal A-P length of the dorsal pons (dP) (Fig. 1*E,F*, *arrow*) was observed, so that the ratio of dP to vP in *Hoxa1*$^{-/-}$ animals, although variable (average ± SEM, 1.45 ± 0.08; $n = 18$), is much larger than in wild-type animals (0.77 ± 0.02; $n = 18$).

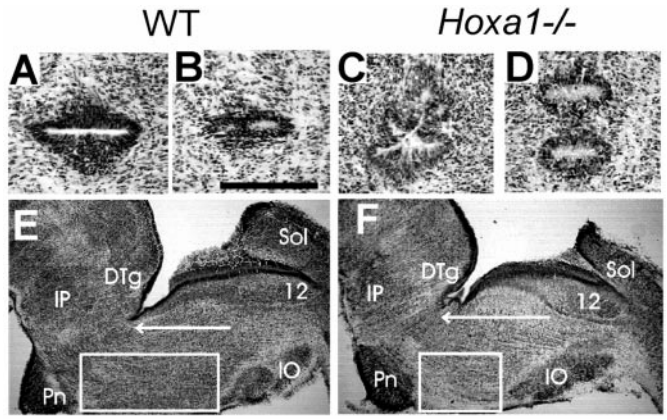

Figure 1. Distinct dorsal and ventral anatomical phenotypes in the *Hoxa1*$^{-/-}$ brainstem at birth. *A–D*, Adjacent horizontal sections showing the ependymal epithelium at the anterior end of the fourth ventricle; *A* and *C* are dorsal to *B* and *D*, respectively. Scale bar, 250 μm. Also see *E* and *F* [caudal to dorsal tegmental area (*DTg*)] and Fig. 2*B* for location. The epithelium forms a single invagination in WT mice (*A*, *B*, *E*), closing in the dorsal pons medially to the trigeminal motor nucleus and forms multiple invaginations (2–5) in *Hoxa1*$^{-/-}$ mice (*C*, *D*, *F*). *E, F*, Parasagittal sections of the hindbrain at P0 in WT (*E*) and *Hoxa1*$^{-/-}$ (*F*) littermates; the A-P length of the pons is affected differently dorsally [*arrow*, from the rostral limit of the hypoglossal nucleus (*12*) to the caudal limit of the *DTg*] and ventrally [*rectangle*, from the rostral pole of the inferior olive (*IO*) to the caudal pole of the pontine nuclei (*Pn*)]. *IP*, Interpeduncular nucleus; *Sol*, solitary nucleus.

We have localized in the dorsolateral pons the anatomical modifications underlying this dP increase. In wild-type mice, caudal to the trigeminal motor nucleus, the parvocellular reticular formation (Rpc-α) (Fig. 2*A,B*, *pc*) normally contains trigeminal premotor interneurons involved in feeding behaviors (Lund et al., 1998). The Rpc-α is likely derived from r3, because it is eliminated in *Krox-20*$^{-/-}$ mutants (Jacquin et al., 1996), in which pontine defects lead to an abnormal suction behavior after birth. In all *Hoxa1*$^{-/-}$ mice ($n = 10$), the anatomy of the Rpc-α is reorganized (Fig. 2) and extended along the A-P axis, in keeping with the abnormalities of the r3-r4 region at early developmental stages (described below) (Carpenter et al., 1993; Mark et al., 1993; Gavalas et al., 1998; Helmbacher et al., 1998; Rijli et al., 1998; Rossel and Capecchi, 1999). In particular, radial stripes of reticular formation and ectopic motoneurons alternate, forming a compound reticular and motor supernumerary neuronal structure (SNS). Most extensive labeling of ectopic SNS motoneurons included three distinct subnuclei (Fig. 2*A,B*) identified by analysis with anti-choline acetyltransferase antibodies. In addition, injecting the fluorescent marker DiI into the trigeminal motor root (Fig. 2*C–F*) revealed that these ectopic subnuclei form a distinct dorsoventral trigeminal motor fasciculus running laterally in the SNS (Fig. 2*D,F*, *asterisks*) caudal to the normal root (Fig. 2*E*, *asterisk*). Therefore, a dP increase in *Hoxa1*$^{-/-}$ mice results from

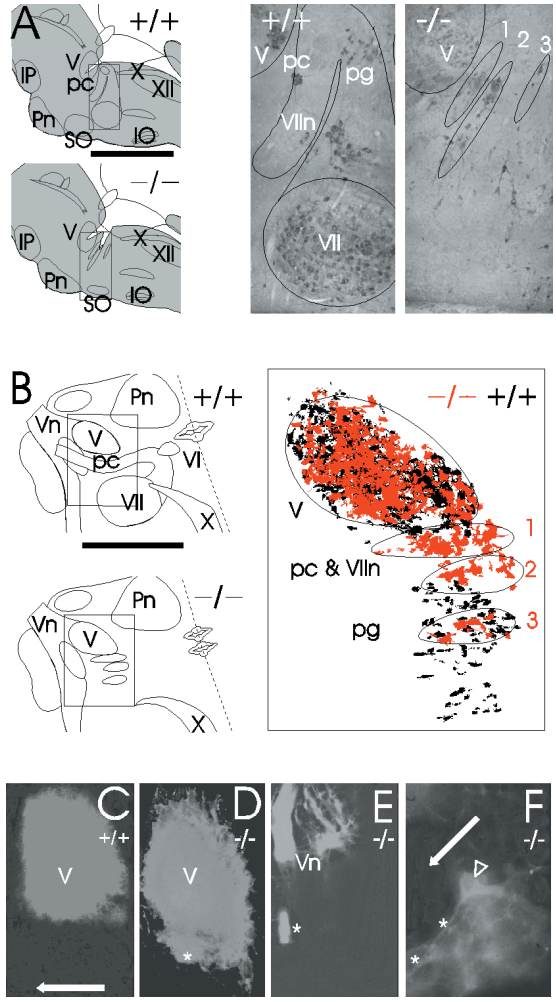

Figure 2. The dorsal anatomical phenotype in *Hoxa1*$^{-/-}$ mice at birth: identification of motoneurons showing location of the SNS. *A*, Sagittal sections of the brainstem, cut parallel to Figure 1*E,F*. The drawings on the *left* (including the analysis of 5 *Hoxa1*$^{-/-}$ mice) include both lateral and medial structures. Scale bar, 1 mm. Medial sections (in *gray*, showing the ventricular surface) are illustrated in Figure 1*E,F*. Note that supernumerary motor (lateral) and ventricular (medial) structures are at the same anteroposterior level of the dorsal pons. Lateral sections (on the *right*) show choline acetyltransferase-immunoreactive WT (+/+) ventral facial structures eliminated by the mutation: the branchial motor nucleus (*VII*), the preganglionic nucleus (*pg*), and accessory nuclei (between VII and pg, extending close to the descending facial root, *VIIn*). In *Hoxa1*$^{-/-}$ mice, caudal to the trigeminal nucleus (*V*), the SNS includes three dorsal motor subnuclei (outlined and numbered) alternating with two unstained stripes of reticular formation. *IO*, Inferior olive; *IP*, interpeduncular nucleus; *pc*, parvocellular reticular formation; *Pn*, pontine nuclei; *SO*, superior olive; *X*, *XII*, dorsal–vagal and hypoglossal motor nuclei. *B*, Horizontal sections cut parallel to the *arrow* in Figure 1*E,F*. Drawings on the *left* (including the analysis of 5 *Hoxa1*$^{-/-}$ mice) show the left part of the pons (scale bar, 1 mm) and the relative positions of the V and VII nuclei and trigeminal nerve root (*Vn*). Close to the midline (*dotted line*), note the appearance of a supernumerary ventricular structure (illustrated in Fig. 1*D*) and elimination of the abducens motor nucleus (*VI*). The *right* part superimposes choline acetyltransferase-immunoreactive pontine neurons in WT (*black*) and *Hoxa1*$^{-/-}$ (*red*) littermates from four horizontal sections sampling, in each littermate, the entire V nucleus and adjacent areas. Supernumerary motor nuclei (*1*, *2*, and *3*) are at the same place as the WT Rpc-α (*pc*), *VIIn*, and *pg*, respectively. *C–E*, Horizontal sections showing retrograde DiI labeling of trigeminal and SNS motoneurons in a WT (*C*; *arrow*, 200 μm) and a *Hoxa1*$^{-/-}$ (*D, E*) mouse. Labeling of the SNS shows the three ectopic trigeminal subnuclei (compare *D* with *C*), and a more ventral view (*E*) shows a supernumerary dorsoventral fasciculus located laterally in subnucleus 2 (*asterisk* in *D* and *E*) and distinct from the WT-like *Vn*. *F*, Medial half of subnucleus 2 at higher magnification (*arrow*, 67 μm, oriented as in *C*; the border of the V is in the *upper left corner*; subnucleus 1 is lacking). The supernumerary motoneuron (*open triangle*) shows an axon (*asterisks*) running in the direction of the lateral fasciculus.

the generation of three additional trigeminal subnuclei alternating with stripes of reticular formation at the same location as the wild-type Rpc-α.

Function of ectopic reticular neurons in the dorsolateral pons of *Hoxa1*$^{-/-}$ mice

To further characterize the reticular cells of the SNS, we investigated their functional connectivity (Fig. 3*G*). The hindbrain was isolated *in vitro* during the first postnatal days [postnatal day 0 (P0) and P1], and the dorsal pons was exposed in a thick horizontal slice (Fig. 3*F*) and made accessible to dorsal approach under microscopic control. This slice preparation also included the bilateral ventral respiratory group (VRG) (Fig. 3*G*, *asterisks*), which generates a persisting rhythmic activity propagating to cranial (e.g., trigeminal) motor neurons from which it can be recorded (Jacquin et al., 1996, 1999). Neuronal populations immediately caudal to the trigeminal nucleus (which in wild type include the Rpc-α premotor neurons) (Fig. 3*G*, *rectangle*) were stimulated by pressure application of the glutamatergic agonist AMPA. The contralateral trigeminal nerve root was recorded to avoid direct stimulation of motoneurons.

AMPA-induced nonrhythmic trigeminal activities recorded from the contralateral trigeminal motor rootlet (the upward noisy deflection of the traces in Figs. 3*A,C*) indicate that normal premotor Rpc-α inputs to the trigeminal motoneurons (Lund et al., 1998) persist in *Hoxa1*$^{-/-}$ mutants. The Rpc-α normally lacks respiratory-related functions. AMPA application had no effect on rhythm frequency in the wild-type preparations (Fig. 3*B*). In the mutants, a robust increase in rhythm frequency is followed in all cases by a transient inhibition of the rhythm (Fig. 3*C,D*). This effect strongly suggests the presence of supernumerary functional efferent connections of the SNS to the rhythm generator, resembling the wild-type ventral pontine respiratory connections, located rostrally to the SNS and originating in r2 and r3 (Jacquin et al., 1996; Borday et al., 1997). Moreover, rhythmic activity recorded from single neurons in the SNS area (Fig. 3*E*) also indicated afferent connections from the rhythm generator. In addition, abnormal axonal pathways were found in the lateral pons by injecting the fluorescent marker DiI into the VRG area (Fig. 3*H–J*). In the mutants, labeling from the VRG revealed a robust axonal pathway (Fig. 3*I*); this pathway was not present in the wild-type (Fig. 3*H*) and ran laterally in the pons. Thus, in *Hoxa1*$^{-/-}$ mice, the SNS exhibits a novel relationship with the respiratory rhythm generator, while preserving premotor connections with the trigeminal system.

Embryological origin of the supernumerary neuronal system

The appearance of this ectopic neuronal system prompts the question of its embryological origin. We investigated the expression of rhombomere-specific molecular markers in *Hoxa1*$^{-/-}$ mutant hindbrains (Fig. 4). Rhombomere-restricted gene expression persists in the ventricular zone after the segmentation period (Wingate and Lumsden, 1996). In 11.5 dpc mutants, expression of the r4 marker *Hoxb1* is drastically reduced and patchy along the dorsoventral axis (Fig. 4, compare *A,B*). To assay for r2 features,

←

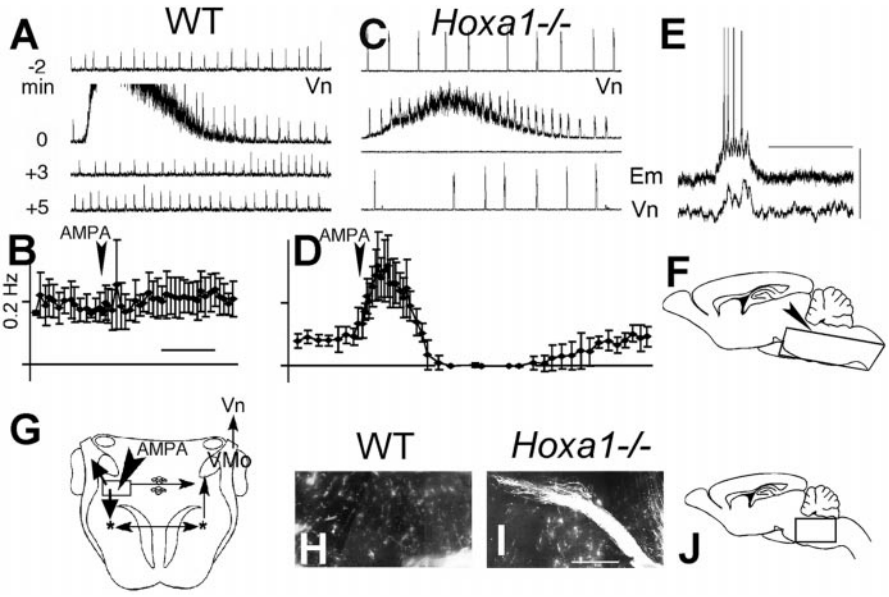

Figure 3. Functional connectivity of reticular neurons in the *Hoxa1*$^{-/-}$ supernumerary neuronal structure at birth. *A–D*, Modification of the contralateral trigeminal nerve activity (*Vn*) induced by exciting SNS neuronal cell bodies using brief (25 msec) pressure applications of AMPA in WT (*A, B*) and *Hoxa1*$^{-/-}$ (*C, D*) hindbrain slices *in vitro*. *A, C*, Four samples of integrated *Vn* activity (2 min long) starting (from *top* to *bottom*) at −2, 0, 3, and 5 min after AMPA application (time indicated on the *left*). In both WT and *Hoxa1*$^{-/-}$ littermates, the rhythm generator produces bursts of activity (fast upward deviations), and AMPA generates background nonrhythmic activity starting at 0 min. *B, D*, Temporal evolution (calibration, 2 min) of average (±SE) burst frequency from five experiments. A significant increase followed by inhibition ($p < 0.001$) indicates a functional connection to the rhythm generator in *Hoxa1*$^{-/-}$ mice but not in WT mice. *E*, *Vn*, Integrated nerve activity; *Em*, membrane potential of a single (*Hoxa1*$^{-/-}$) neuron located in the SNS area (scale bars, 20 mV, 1 sec). A connection from the rhythm generator results in a simultaneous *Vn* burst and neuronal depolarization inducing firing of action potentials. *F, G*, Schematic presentation of the slice preparation in sagittal (*F*, *arrowhead* indicates the top side) and horizontal (*G*) sections. The *rectangle* in *G* indicates the approximate extent of the area affected by AMPA applications, indicated by the *arrowhead*; more medial applications were ineffective. *Thin arrows* indicate WT projections, preserved in mutants; these are either rhythmic, from the bilateral rhythm generator (*asterisks*) to the contralateral trigeminal nucleus (*VMo*) and *Vn* (recorded), or nonrhythmic premotor neurons from Rpc-α/SNS to *VMo*. *Thick arrows* indicate supernumerary connections in mutants, including those from the SNS to the rhythm generator and the trigeminal axons of SNS motoneurons. *H–J*, Sagittal sections (location in *J*, rostral to the *left*) of the most lateral 300 μm of the pons showing in mutant (*I*) but not in WT (*H*) animals, an axonal fasciculus stained after DiI injection in the area of the rhythm generator (*bottom right corner*). Scale bar, 200 μm.

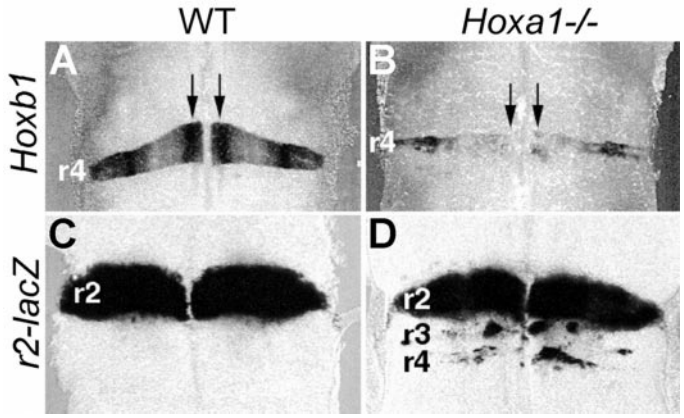

Figure 4. Molecular and morphological patterning defects in a *Hoxa1* mutant hindbrain. A dorsal view of 11.5 dpc WT (*A, C*) and *Hoxa1*$^{-/-}$ (*B, D*) mutant hindbrains hybridized with the r4-specific *Hoxb1* (*A, B*) or carrying a *lacZ* reporter under the control of an r2-specific enhancer (*C, D*) is shown. *Vertical arrows* indicate the location of the motoneuron progenitor columns.

we generated a transgenic line containing the *lacZ* reporter under the control of a *Hoxa2* r2-specific enhancer (Frasch et al., 1995) (Fig. 4*C*). In *Hoxa1*$^{-/-}$ mutants, ectopic patches of cells expressing the r2 marker are present at the r4 axial level (Fig. 4, compare *C,D*); this is remarkably similar to what is observed in *Hoxb1*$^{-/-}$ mice (Studer et al., 1996). In addition, patches of r2-like cells are also present at the r3 level, as described previously (Helmbacher et al., 1998). Thus, in the absence of *Hoxa1*, some neural precursors at the presumptive r3-r4 levels fail to activate or properly maintain their appropriate molecular programs and acquire an r2 identity.

To investigate the developmental fate of these ectopic r2-like precursors, we examined motoneuron development in the hindbrain of *Hoxa1*$^{-/-}$ mice. In wild-type 11.5 dpc embryos, the *Phox2b* gene is expressed in migrating motoneurons (Pattyn et al., 1997). *Phox2b* expression in ventral r4 identifies facial motoneurons migrating caudally through r5 into r6 (Fig. 5*A*, *bent arrow*) to form the facial (VIIth) motor nucleus, whereas strings of *Phox2b*-positive cells in r2 are indicative of dorsal migration of trigeminal motoneurons (Fig. 5*A*, *straight arrows*). In the *Hoxa1*$^{-/-}$ mutant r4 region (Fig. 5*B*), a much reduced, although not abolished, *Phox2b* expression identifies a small number of facial motoneurons migrating caudally (Fig. 5*B*, *bent* and *dashed arrow*). In addition, an abnormal trigeminal-like lateral migration of cells can be detected (Fig. 5*B*, *straight arrows*) that is completed at ~12.5 dpc (Fig. 5*D*) and results in a characteristic dorsolateral accumulation of ectopic *Phox2b*-positive cells (Fig. 5, *rectangle*, compare *C,D*). This population includes ectopic motoneurons as assessed by anti-Islet1 immunohistochemistry (Fig. 5, *arrows*, compare *E,F*). Remarkably, lack of caudal migration of facial motoneurons and lateral trigeminal-like migration are also observed in *Hoxb1*$^{-/-}$ mice (Studer et al., 1996). Thus, together with the above molecular analysis (Fig. 4), these data suggest facial-to-trigeminal changes in motoneuron subtype identity in *Hoxa1* mutants that could be induced by lack of *Hoxb1* activation in pre-r4 cells.

Persistence and functional role of the supernumerary neuronal system after birth

To investigate the functional role of the SNS in controlling respiratory and feeding rhythms *in vivo*, we have compared mutant and wild-type behaviors in relation to the anatomical modification of the pons. Although irregular after birth, the wild-type minute ventilation increases progressively and stabilizes at the end of the first day (Fig. 6*A*, *left*). In contrast, mutants exhibited a variable neonatal respiratory frequency (NRF) 2–4 hr after

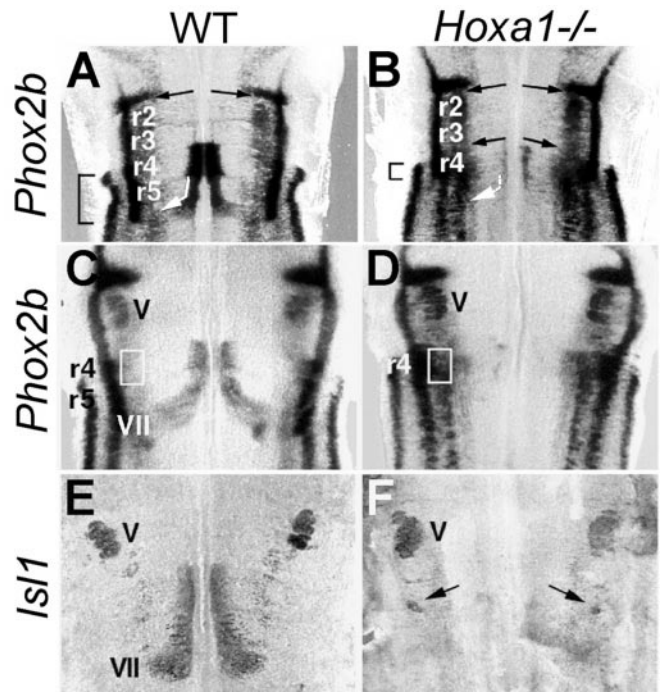

Figure 5. The *Hoxa1*$^{-/-}$ supernumerary motoneurons: migration and final postnatal location. A dorsal view of 11.5 (*A, B*) and 12.5 (*C–F*) dpc WT and *Hoxa1*$^{-/-}$ mutant hindbrains, respectively, flat-mounted and hybridized with *Phox2b* (*A–D*) or *Isl1* (*E, F*) probes is shown. The *bent white arrow* in *A* and *B* indicates caudal migration of facial (VII) motoneurons. The *straight arrows* in *A* and *B* indicate dorsal migration of trigeminal (V) motoneurons and, in *Hoxa1*$^{-/-}$ mice (*B*), of supernumerary motoneurons from r4. The *rectangles* in *C* and *D* and the *arrows* in *F* indicate ectopic, dorsolateral accumulation of *Phox2b*- and *Isl1*-positive cells, which was not present in WT mice.

birth and eventually apneic breathing and death (Fig. 6*A*, *right*). A correlation was found in mutants between the NRF and the hindbrain anatomical index dP/vP ($r = 0.83$ vs $r = 0.32$ in wild-type mice) (Fig. 6*B*), indicating that there are pontine abnormalities accelerating spontaneous breathing at birth. In contrast, the suction behavior, estimated by the frequency of jaw openings induced by a buccal stimulus (Jacquin et al., 1996), was normal in the mutants and unrelated to dP/vP ($r = 0.25$). In addition, *Hoxa1*$^{-/-}$ newborns with a low NRF (<35 breaths/min; $n = 7$) died within 2.5 ± 0.8 hr (Fig. 6*C*, *bottom left triangles*), whereas those exhibiting a higher NRF ($n = 15$) progressively increased their respiratory rate to normal values (Fig. 6*A,C*) and survived for 18 ± 7 hr. Thus, one possibility is that the appearance of the SNS may result in enhanced survival rates by significantly increasing NRF values, so that the rhythm promoting action of the SNS seems to compensate for the lethal apneic breathing resulting from vP hypoplasia. To further investigate this hypothesis, animals with the highest NRF were submitted to naloxone administration, a treatment known to be effective on life-threatening pathologies resulting from the vP hypoplasia (for example, in *Krox-20*$^{-/-}$ mutants) (Jacquin et al., 1996). A striking effect of naloxone administration was obtained in two of the five treated *Hoxa1*$^{-/-}$ newborns (Fig. 6*C*, *filled circles*); one of them survived 4 d, whereas the other was killed 12 d after birth. Interestingly, in this animal, histological analysis revealed the same pattern of SNS motoneurons (Fig. 6*D*) that was observed at birth (Fig. 2). The survival of these motoneurons is noteworthy, considering the wave of apoptosis that normally removes abnormal motoneurons in the fetal hindbrain before birth (deLapeyrière and Henderson, 1997). Altogether, the present *in vitro* and *in vivo* observations demonstrate that the *Hoxa1* mutation results in the incorporation of a SNS, which originates from the mutant r3-r4 region, into the hindbrain neural network. As a consequence, the animal acquires a novel respiratory-related function enhancing survival, while not affecting suction, a function that is under the control of neuronal populations from the same region.

DISCUSSION

These results allow a hypothesis that is compatible with the involvement of developmental control genes in the assembly of functional neuronal circuits (Tanabe and Jessell, 1996; Brunet and Ghysen, 1999). In fact, this work provides the first formal evidence that selective modification of the expression pattern of a *Hox* gene whose expression is transient in the presumptive hindbrain, namely *Hoxa1*, is sufficient to incorporate a novel functional neural circuit in the mature hindbrain. This striking finding prompts the question of the cascade of regulatory events triggered by *Hoxa1* loss-of-function, leading to long-term modification of hindbrain neural networks. Previous work demonstrated a role for *Hoxa1* in the activation of *Hoxb1* expression in the presumptive r4 (Studer et al., 1998). Thus, some of the long-term effects of the *Hoxa1* mutation could be attributable to the lack of *Hoxb1* activation in a subset of presumptive r4 cells, leading to r2-like specification. However, *Hoxa1*, unlike *Hoxb1*, appears to

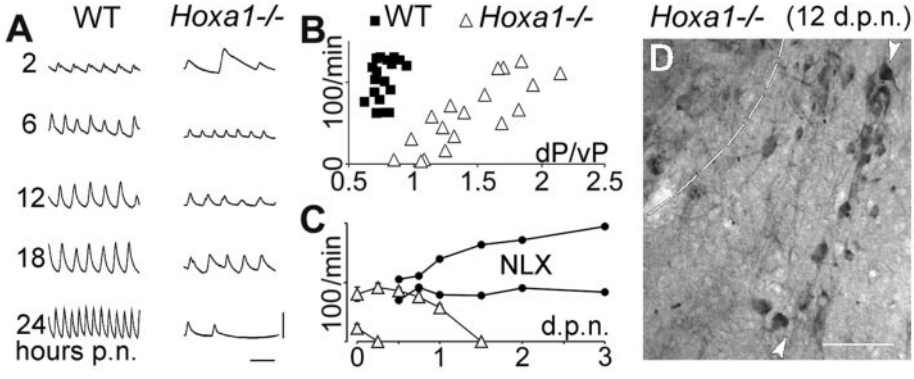

Figure 6. The *Hoxa1*$^{-/-}$ breathing pattern after birth. *A*, Samples of plethysmographic recording (inspiration upwards) 2, 6, 12, 18, and 24 hr after birth [postnatally (*p.n.*)] showing normal maturation in a WT mouse and transient increase of frequency in a mutant mouse. Calibration: 20 μl, 1 sec. The mutant animal typically exhibits irregular breathing at birth (*top trace*) and eventually apneic breathing and death (*bottom trace*). *B*, Individual *Hoxa1*$^{-/-}$ (*open triangles*) and WT (*filled squares*) mice identified by their respiratory rate at birth (ordinates) and the dP/vP index quantifying the abnormality of the pontine A-P distances [see *arrow* (dP) and *rectangle* (vP) in Fig. 1*E,F*]. A correlation exists in *Hoxa1*$^{-/-}$ mice but not in WT mice. *C*, Temporal evolution of average respiratory frequency (±SEM) in *Hoxa1*$^{-/-}$ animals breathing faster or slower than 35 breaths/min at birth (*open triangles*). The slowest animals lack the rhythm stimulation shown in *A* (6–18 hours p.n.); the fastest animals survive longer; death was delayed by >3 days postnatally (*d.p.n.*)] in two animals (*filled circles*) treated with subcutaneous naloxone (*NLX*). *D*, Supernumerary motoneurons in a *NLX*-treated animal killed 12 d after birth. The sagittal section (rostral to the *left*) shows choline acetyltransferase-immunoreactive motoneurons (*arrowheads*) caudal to the trigeminal motor nucleus (located in the *top left corner*). Scale bar, 100 μm.

control both r4 and, indirectly, r3 development (Helmbacher et al., 1998) (this study). Thus, it is tempting to speculate that regulatory changes in two adjacent rhombomeres may be required for the generation of a SNS. Interestingly, we have shown recently that assembling of a rhythm-promoting respiratory network also requires a two-segment functional unit in the chick (Fortin et al., 1999). In this respect, it will be interesting to compare the physiology of neuronal networks in *Hoxb1*$^{-/-}$ mutants with that of *Hoxa1*$^{-/-}$ mutants.

Because hindbrain neurons control adaptive behaviors, these findings have considerable significance both on developmental and evolutionary grounds. The evolution of neural networks of multisegmental origin may be facilitated by the partitioning of the early hindbrain in a number of metameric units initially developing as independent modules (Lumsden, 1990; Clarke and Lumsden, 1993; Champagnat and Fortin, 1996). As a result, subsets of neurons may be developmentally isolated from each other and allowed to evolve independently. Our present data suggest that *Hox* genes may provide a genetic basis for segment-specific modulation of neuronal development and connectivity. Changes in *Hox cis*-regulatory modules and downstream targets have been suggested to underlie morphological changes of segmented structures in animal evolution (Gellon and McGinnis, 1998). Similarly, local changes in the regulation of *Hox* genes within the segmented hindbrain of vertebrates may offer novel opportunities for the evolution of distinct subsets of neurons, without affecting the function of others, eventually resulting in novel functional features (Brunet and Ghysen, 1999). In this respect, studies of conditional segment-specific *Hox* mutations, which may not result in lethality of the animal, will be important to further investigate adaptive mechanisms in the development of hindbrain neuronal networks.

REFERENCES

Bell E, Wingate RJ, Lumsden A (1999) Homeotic transformation of rhombomere identity after localized *Hoxb1* misexpression. Science 284:2168–2171.

Borday V, Kato F, Champagnat J (1997) A ventral pontine pathway promotes rhythmic activity in the medulla of neonate mice. NeuroReport 8:3679–3683.

Brunet JF, Ghysen A (1999) Deconstructing cell determination: proneural genes and neuronal identity. Bioessays 21:313–318.

Carpenter EM, Goddard JM, Chisaka O, Manley NR, Capecchi MR (1993) Loss of *HoxA1* (*Hox-1.6*) function results in the reorganization of the murine hindbrain. Development 118:1063–1075.

Champagnat J, Fortin G (1996) Primordial respiratory-like rhythm generation in the vertebrate embryo. Trends Neurosci 20:119–124.

Clarke JD, Lumsden A (1993) Segmental repetition of neuronal phenotype sets in the chick embryo hindbrain. Development 118:151–162.

Davenne M, Maconochie MK, Neun R, Pattyn A, Chambon P, Krumlauf R, Rijli FM (1999) *Hoxa2* and *Hoxb2* control dorsoventral patterns of neuronal development in the rostral hindbrain. Neuron 22:677–691.

deLapeyrière O, Henderson CE (1997) Motoneuron differentiation, survival, and synaptogenesis. Curr Opin Genet Dev 7:642–650.

Fortin G, Jungbluth S, Lumsden A, Champagnat J (1999) Segmental specification of GABAergic inhibition during development of hindbrain neural networks. Nat Neurosci 2:873–877.

Fortin G, Domínguez del Toro E, Abadie V, Guimarães L, Foutz AS, Denavit-Saubié M, Rouyer F, Champagnat J (2000) Genetic and developmental models for the neural control of breathing in vertebrates. Respir Physiol 122:247–257.

Frasch M, Chen X, Lufkin T (1995) Evolutionary-conserved enhancers direct region-specific expression of the murine *Hoxa-1* and *Hoxa-2* loci in both mice and *Drosophila*. Development 121:957–974.

Gavalas A, Davenne M, Lumsden A, Chambon P, Rijli FM (1997) Role of *Hoxa-2* in axon pathfinding and rostral hindbrain patterning. Development 124:3683–3691.

Gavalas A, Studer M, Lumsden A, Rijli FM, Krumlauf R, Chambon P (1998) *Hoxa1* and *Hoxb1* synergize in patterning the hindbrain, cranial nerves, and second pharyngeal arch. Development 125:1123–1136.

Gellon G, McGinnis W (1998) Shaping animal body plans in development and evolution by modulation of *Hox* expression patterns. Bioessays 20:116–125.

Goddard JM, Rossel M, Manley NR, Capecchi MR (1996) Mice with targeted disruption of *Hoxb-1* fail to form the motor nucleus of the VIIth nerve. Development 122:3217–3228.

Helmbacher F, Pujades C, Desmarquet C, Frain M, Rijli FM, Chambon P, Charnay P (1998) *Hoxa1* and *Krox-20* synergize to control the development of rhombomere 3. Development 125:4739–4748.

Jacquin TD, Borday V, Schneider-Maunoury S, Topilko P, Ghilini G, Kato F, Charnay P, Champagnat J (1996) Reorganisation of pontine rhythmogenic neuronal networks in *Krox-20* knockout mice. Neuron 17:747–758.

Jacquin TD, Sadoc G, Borday V, Champagnat J (1999) Pontine and medullary control of the respiratory activity in the trigeminal and facial nerves of the newborn mouse: an in vitro study. Eur J Neurosci 11:213–222.

Jungbluth S, Bell E, Lumsden A (1999) Specification of distinct motor neuron identities by the singular activities of individual *Hox* genes. Development 126:2751–2758.

Lumsden A (1990) The cellular basis of segmentation in the developing hindbrain. Trends Neurosci 13:329–335.

Lumsden A, Krumlauf R (1996) Patterning the vertebrate neuraxis. Science 274:1109–1115.

Lund JP, Kolta A, Westberg KG, Scott G (1998) Brainstem mechanisms underlying feeding behaviors. Curr Opin Neurobiol 8:718–724.

Mark M, Lufkin T, Vonesh JL, Ruberte E, Olivo JC, Dollé P, Gorry P, Lumsden A, Chambon P (1993) Two rhombomeres are altered in *Hoxa-1* mutant mice. Development 119:319–338.

Murphy P, Hill RE (1991) Expression of the mouse labial-like homeobox-containing genes, *Hox 2.9* and *Hox 1.6*, during segmentation of the hindbrain. Development 111:61–74.

Pattyn A, Morin X, Cremer H, Goridis C, Brunet JF (1997) Expression and interactions of the two closely related homeobox genes *Phox2a* and *Phox2b* during neurogenesis. Development 124:4065–4075.

Rijli FM, Gavalas A, Chambon P (1998) Segmentation and specification in the branchial region of the head: the role of the *Hox* selector genes. Int J Dev Biol 42:393–401.

Rossel M, Capecchi MR (1999) Mice mutant for both *Hoxa1* and *Hoxb1* show extensive remodeling of the hindbrain and defects in craniofacial development. Development 126:5027–5040.

Studer M, Lumsden A, Ariza-McNaughton L, Bradley A, Krumlauf R (1996) Altered segmental identity and abnormal migration of motor neurons in mice lacking *Hoxb-1*. Nature 384:630–634.

Studer M, Gavalas A, Marshall H, Ariza-McNaughton L, Rijli FM, Chambon P, Krumlauf R (1998) Genetic interactions between *Hoxa1* and *Hoxb1* reveal new roles in regulation of early hindbrain patterning. Development 125:1025–1036.

Tanabe Y, Jessell TM (1996) Diversity and pattern in the developing spinal cord. Science 274:1115–1123.

Wingate RJT, Lumsden A (1996) Persistence of rhombomeric organisation in the postsegmental hindbrain. Development 122:2143–2152.